Synthesis and photocatalytic activity of WO_3 nanocomposites incorporating GO and MWCNTs for enhanced Rhodamine-B degradation

Hatel, Rhizlane; Boukhoubza, Issam; Derkaoui, Issam; Kabatas, Mohamed A.Basyooni M.; Matei, Elena; Enculescu, Monica; Baitoul, Mimouna

DOI
10.1016/j.colsurfa.2025.136395

Publication date
2025

Document Version
Final published version

Published in
Colloids and Surfaces A: Physicochemical and Engineering Aspects

Citation (APA)
Hatel, R., Boukhoubza, I., Derkaoui, I., Kabatas, M. A. B. M., Matei, E., Enculescu, M., & Baitoul, M. (2025). Synthesis and photocatalytic activity of WO_3 nanocomposites incorporating GO and MWCNTs for enhanced Rhodamine-B degradation. *Colloids and Surfaces A: Physicochemical and Engineering Aspects*, *711*, Article 136395. https://doi.org/10.1016/j.colsurfa.2025.136395

Colloids and Surfaces A: Physicochemical and Engineering Aspects 711 (2025) 136395

Contents lists available at ScienceDirect

Colloids and Surfaces A: Physicochemical and Engineering Aspects

journal homepage: www.elsevier.com/locate/colsurfa

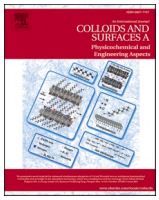

Synthesis and photocatalytic activity of WO_3 nanocomposites incorporating GO and MWCNTs for enhanced Rhodamine-B degradation

Rhizlane Hatel [a,1], Issam Boukhoubza [b,c,1], Issam Derkaoui [c], Mohamed A. Basyooni-M. Kabatas [d,e,*], Elena Matei [b], Monica Enculescu [b], Mimouna Baitoul [c]

[a] Laboratory of Applied Physics, Informatics and Statistics (LPAIS), University Sidi Mohammed Ben Abdellah, Faculty of Sciences Dhar El Mahraz, Fez. B.P. 1796, Morocco
[b] National Institute of Materials Physics, Atomistilor 405A, Magurele 077125, Romania
[c] Laboratory of Solid State Physics, Faculty of Sciences Dhar el Mahraz, University Sidi Mohammed Ben Abdellah, PO Box 1796, Atlas Fez 30 000, Morocco
[d] Department of Precision and Microsystems Engineering, Delft University of Technology, Mekelweg 2, Delft 2628 CD, the Netherlands
[e] Department of Nanotechnology and Advanced Materials, Graduate School of Applied and Natural Science, Selçuk University, Konya 42030, Turkey

GRAPHICAL ABSTRACT

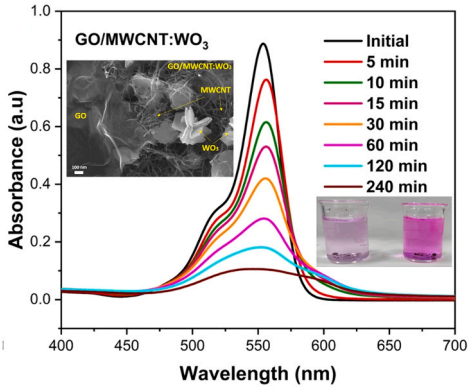

ARTICLE INFO

Keywords:
Ternary nanocomposite
Photocatalysis
Graphene oxide sheets
Tungsten trioxide

ABSTRACT

In this study, we developed a ternary nanocomposite using graphene oxide (GO), multiwalled carbon nanotubes (MWCNTs), and tungsten trioxide (WO_3), nanostructures, synthesized via a straightforward chemical process with ultrasound assistance. The initial composition was GO/MWCNT, later combined with WO_3 to form the GO/MWCNT: WO_3 (25/25:50) structure. Characterization was performed using X-ray diffraction, which revealed the multiphase nature of the WO_3 nanostructures. Scanning Electron Microscopy showed the one-dimensional CNTs interwoven with graphene oxide sheets decorated with densely populated WO_3 nanopetals. Fourier transform infrared and Raman spectroscopy confirmed the chemical composition of the system. The photocatalytic degradation of Rhodamine-B in water under visible light irradiation was significantly enhanced using the GO/

* Corresponding author at: Department of Precision and Microsystems Engineering, Delft University of Technology, Mekelweg 2, Delft 2628 CD, the Netherlands.
E-mail addresses: m.kabatas@tudelft.nl, m.a.basyooni@gmail.com (M.A.B.-M. Kabatas).
[1] Authors contributed equally

https://doi.org/10.1016/j.colsurfa.2025.136395
Received 13 December 2024; Received in revised form 1 February 2025; Accepted 10 February 2025
Available online 10 February 2025

MWCNT: WO_3 nanocomposite, achieving an 85 % degradation rate compared to only 10 % by GO alone, highlighting its potential for environmental remediation.

1. Introduction

Today's industry has modernized and advanced and is considered an engine of economic growth. Unfortunately, it generates various wastes that destroy the environment with discharges heavily contaminated with organic pollutants [1]. Dyes are among the most dangerous contaminants in many industrial sectors, such as food, cosmetics, and clinical products, particularly in the textile industries. The molecules of these dyes are complex to biodegrade or degrade by conventional methods [2]. Rhodamine B is an intense red xanthene dye widely used in pharmaceutical and cosmetic preparations [3]. This dye is water soluble and highly toxic even in low concentrations. Its accumulation in aquatic environments has posed dangerous adverse effects, including irritation, carcinogenicity, and neurotoxicity, highlighting the urgent need for efficient, cost-effective, and environmentally friendly treatment methods [4].

Several physical, chemical, and biological technologies have successfully been developed to control pollution [5]. Most of these technologies were based on analysis/photocatalysis applications [6]. Currently, many different materials have been used as photocatalysts. Among these materials, nanocomposites based on nanocarbon and metal oxide nanostructures have aroused an enormous interest due to the cooperative effects between both components [6,7]. According to recent reviews, authors have developed various techniques to utilize carbon's tubular and planar forms, namely carbon nanotubes and graphene, for efficient dye removal from aqueous environments. Graphene derivatives have large surface areas, chemical stability, high adsorption capacity, and numerous available functional groups. CNT exhibits low density, large surface area, and exceptional electrical properties. These characteristics enable them to provide impressive water treatment performance, driven by their strong affinity for toxic organic and inorganic pollutants [8,9].

Many studies have focused more on functionalizing carbon materials with various types of nanostructured metal oxide, producing newer materials to continue to boost their performances [10]. Wang et al. used graphene/CNTs hybrid as the composite support of TiO_2, which significantly enhanced the photocatalytic performance in the degradation of MB dye under UV light irradiation [11]. Unlike TiO_2, tungsten trioxide (WO_3) with a band gap of 2.8 eV is a promising material due to its polymorphism phenomenon by adopting different crystallographic structures and efficiently utilizing visible light [12]. Combined with the graphene/CNT hybrid, extending the absorption range to the visible region and effectively promoting environmental remedy might be advantageous.

Herein, the prime novelty of this study is the preparation of low-cost ternary nanocomposites (GO/MWCNT: WO_3) and the investigation of the synergetic effects between the different kinds of components aiming to improve the photocatalytic activity for the removal of RhB dyes from aqueous solution. The prepared samples were characterized by X-ray diffraction (XRD), Scanning electron microscopy using mapping and EDX, Fourier transform infrared (FTIR), and RAMAN spectroscopy to determine the chemical composition and confirm the successful preparation of the ternary nanocomposite. Under visible light, degrading Rhodamine B has explored the photocatalytic efficiency of GO/MWCNT: WO_3.

2. Experimental

2.1. Materials

Multiwalled carbon nanotubes used in this study were provided by Arkema. The powder of tungsten carbide (WC) and graphite powder, used as the initial precursors, were purchased from Sigma-Aldrich. Rhodamine B (RhB, $C_{28}H_{31}ClN_2O_3$), H_2SO_4, $KMnO_4$, and DMF were obtained from Merck, Germany. All chemicals were used as received, and no further purification was needed.

2.2. Preparation of GO/MWCNT

GO is synthesized from pure graphite and treated with H_2SO_4 and $KMnO_4$ using the modified Hummers method [13]. The carbon nanotubes were dispersed in a DMF solution and ultrasonicated for 1 h to increase their dispersion/solubility and homogeneity in the aqueous solution of GO. The two previously prepared solutions of GO and MWCNT are mixed and ultrasonicated for 2 h to obtain a homogeneous solution, with a mass ratio of 1:1 for MWCNT: GO.

2.3. Preparation of ternary nanocomposite of GO/MWCNT: WO_3

In a typical preparation (Fig. 1), the calculated amount of $WO_3 \cdot H_2O$ prepared in our previous work [14] was dispersed in water and was added to GO/MWCNT solution with a weight ratio (25/25:50). The mixed solution was stirred for 1 h and ultrasonicated for 30 min. The obtained precipitation was filtrated, dried at 60 °C overnight, and treated at 200 °C for 2 h.

2.4. Characterization techniques

Morphology observation was carried out by scanning electron microscopy (SEM) using a Gemini 500 from Carl Zeiss, equipped with an

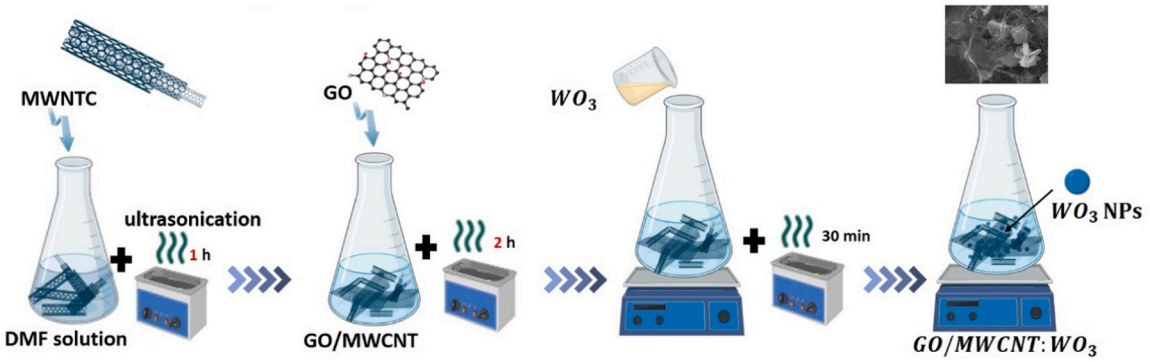

Fig. 1. Representation of GO/MWCNT and GO/MWCNT: WO_3 nanocomposites growth.

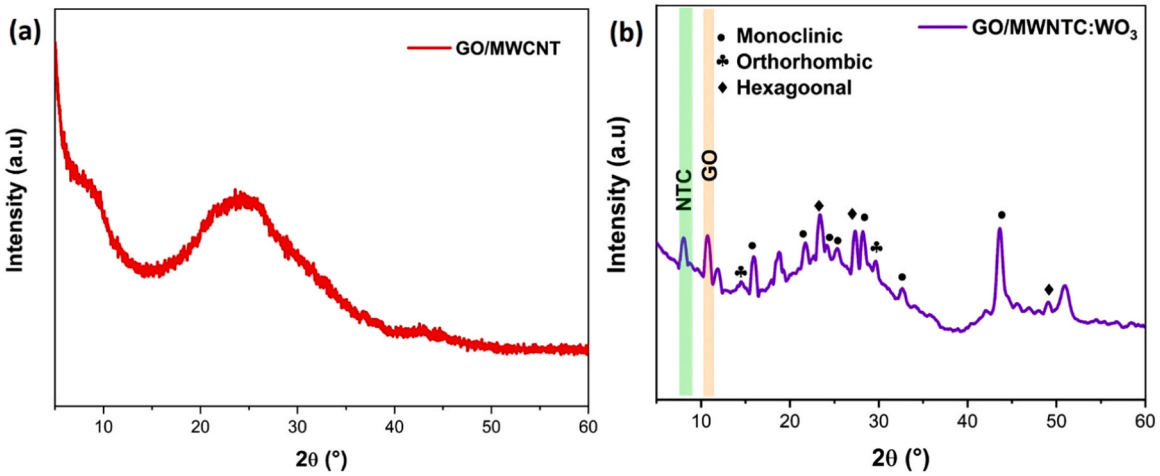

Fig. 2. X-ray diffraction (XRD) patterns: (a) GO/MWCNT and (b) GO/MWCNT: WO_3 nanocomposites.

energy-dispersive X-ray spectrometer (EDX) from Bruker. The crystalline structures of the prepared samples were investigated through X-ray diffraction (XRD) using a Bruker diffractometer with CuKα radiation. Fourier Transform Infrared spectra (FT-IR) were recorded at room temperature in the transmittance mode using a Vertex 70 spectrophotometer, with a resolution of 4 cm^{-1} over a wavenumber range of 400–4000 cm^{-1}. Raman scattering spectra were recorded using LabRAM HR Evolution Raman spectrometer equipped with an excitation wavelength of 663 nm.

To evaluate the photocatalytic degradation performance of GO and GO/MWCNT: WO_3 nanocomposite at room, 0.5 mg of the prepared photocatalysts were dispersed into a flask containing 10 mL of RhB aqueous solution (10^{-5} M) at pH= 7. The temperature was maintained at 25 °C, and the suspension was stirred in the dark for 30 min to achieve the adsorption-desorption equilibrium between the catalyst and organic RhB dye. Then, the solution was irradiated with white light for 240 min using an SF300-A Small Collimated Beam Solar Simulator (Sciencetech, London, ON, Canada) equipped with an Air Mass AM1.5 G Filter (spot size: 25 mm diameter at one Sun) and an integrated electrical shutter with a controller and a Xe lamp (300 W). At different intervals, a specific volume of the solutions was taken during the degradation process. The optical absorbance spectra were recorded in the range of 200–700 nm using UV–Vis–NIR CARY 5000 (Varian, Agilent Technologies Deutschland GmbH, Waldbronn, Germany) spectrophotometer provided with a quartz cell with a light path of 10 mm.

3. Results and discussion

3.1. X-ray diffraction

Fig. 2a shows the X-ray diffraction spectrum of GO nanosheets functionalized by MWCNTs that were previously dispersed in an aqueous solution of DMF. The disappearance of the characteristic peak of GO (11.26°) and the broad diffraction peak observed at 25.8° corresponds to both MWCNTs and partially reduced GO (RGO) [15]. This XRD spectrum shows the combined structure of nanosheets and nanotubes, indicating the successful exfoliation of GO nanosheets. In this preparation, the modification of the surface of the MWCNTs by the DMF made it possible to improve the dispersion of the MWCNTs in the aqueous GO solution. As a result, the interactions between the two components prevent the stacking of graphene sheets and keep the dispersion of GO / MWCNT more stable.

Fig. 2b shows the typical X-ray diffraction spectrum of GO/MWCNT: WO_3 nanocomposite. It can be seen that the spectrum is dominated by the trace of the GO/MWCNT system, which confirms the preservation of the GO/MWCNT homogeneity and exfoliated structure even after the combination with the WO_3 nanostructures. The appearance of multiple diffraction peaks corresponding to WO_3 confirms the existence of a mixture of crystallographic phases, including the monoclinic, hexagonal, and orthorhombic phases [16]. This is probably due to the diversity of the elements within the nanocomposite, which could disturb the crystal structure as well as the electronic structure of the nanomaterials.

3.2. Scanning electron microscopy

The SEM technique was used to observe the surface condition of nanocarbons and to more clearly follow the effect of the combination of GO/MWCNT: WO_3 materials on the resulting nanocomposite morphology. In the SEM image in Fig. 3a-d, the existence of the nanosheet and nanotube morphologies is apparent, confirming the successful preparation of the GO/MWCNT. The presence of nanoparticles of WO_3 can be observed in the form of short-fused nano petals entangled into the GO/MWCNT matrix. In our previous work for GO: WO_3 (50:50), we obtained GO nanosheets functionalized with rod-like shape WO_3 [17]. Therefore, this result highlights the effect of the incorporation of MWCNT on the modification of the metal oxide morphology.

The elemental composition of the as-prepared nanocomposite was determined by EDX microanalysis, and the results are shown in Fig. 3e, f. The results obtained from EDX mapping images confirmed that the nanocomposite was enriched in elements such as W, O, and C. They revealed the homogeneous distribution of elements within the ternary systems, which implies the successful combination and functionalization.

3.3. FTIR and Raman analysis

FTIR analyses of GO/MWCNT and GO/MWCNT: WO_3 nanocomposite were described as given in Fig. 4. the spectrum of GO/MWCNT (Fig. 4a) exihibit several characteristic bands of oxygenated functional groups [17]. The broad band near 3420 cm^{-1} is related to the stretching vibration mode of -OH rising from hydroxyl groups and the physically adsorbed H_2O. The band at 1610 cm^{-1} characteristic of the binding C═C corresponding to the graphitic plans constituting GO and MWCNT, respectively. The bands near 1252 cm^{-1} and 1060 cm^{-1} were considered to the O-H deformation vibration, C-O (epoxy) and C-O (alkoxy) stretching vibration, respec- tively [18].

Fig. 4b shows the infrared spectrum of the ternary GO/MWCNT: WO_3 nanocomposite. Close examinations reveal the absence of the bands attributed to the modes of vibration of the bonds (–OH), which the thermal treatment could explain. Compared with WO_3 alone in our previous work [16], the appearance of specific bands in the low-frequency zone was due to the change in binding angles and/or

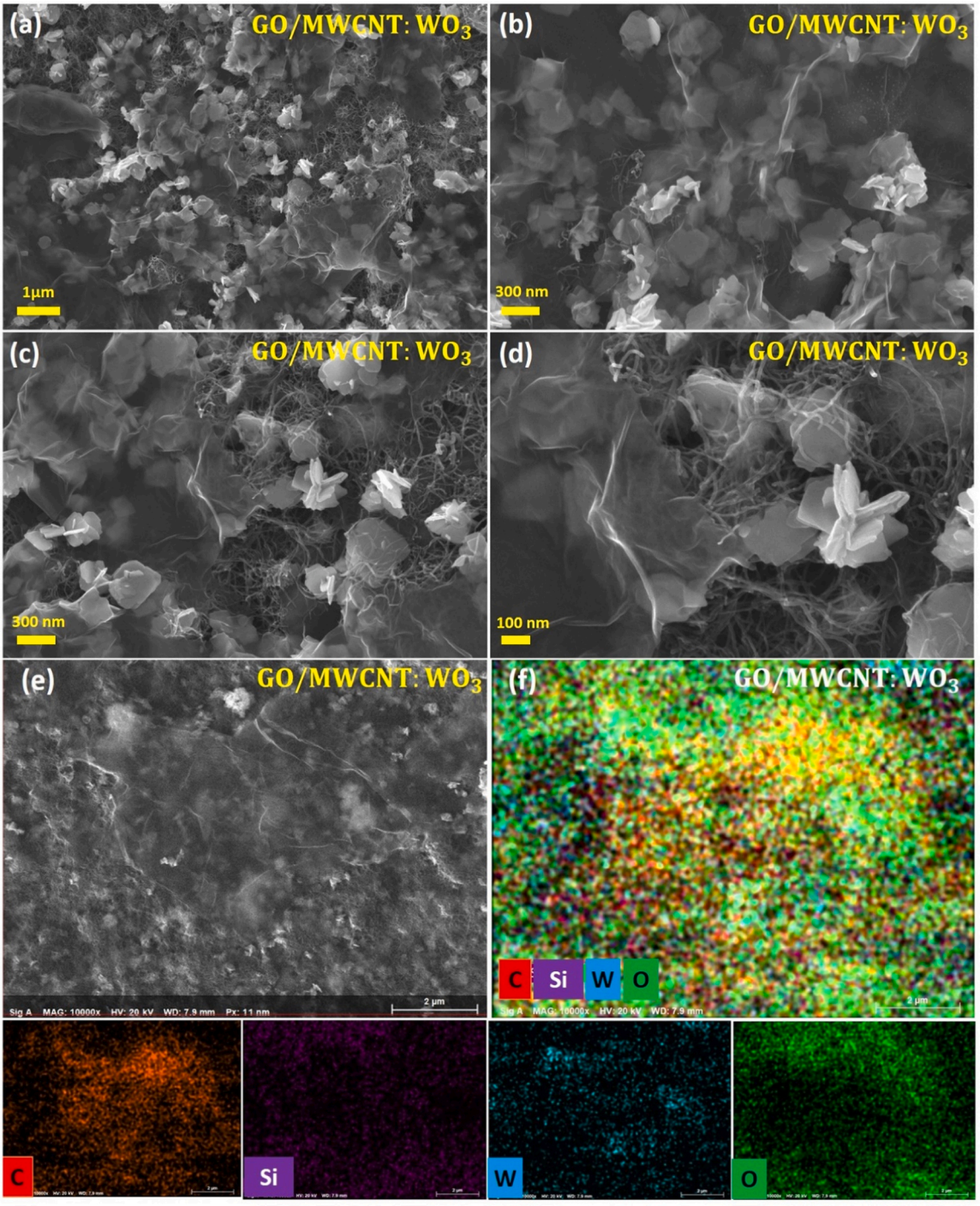

Fig. 3. (a-d) SEM images with different magnifications and (e, f) EDX maps of GO/MWCNT: WO_3 nanocomposite.

binding lengths of WO_6 octahedra after the combination between WO_3 and GO/MWCNT. Studies have reported that the distortion of octahedra and the considerable lowering of symmetry in the structure lead to many active modes in FTIR and Raman Spectroscopy [19]. This is in agreement with the results obtained by the XRD. Moreover, the band at about 1120 cm^{-1} could be attributed to the W-O-C bond. This result suggests that the bond between the constituents is in the form of a covalent functionalization.

Raman spectroscopy was used as a complementary FTIR technique to confirm the successful combination. It is well known that the low-frequency region is the most Raman-studied part of any metal oxide. Consequently, all the bands in this region are related to WO_3 nanostructures. The Raman spectrum of GO/MWCNT: WO_3 nanocomposite exhibits vibrations located at 200–400 and 600–900 cm-1, respectively, corresponding to the deformation and stretching modes. The strongest bands at 807 and 675 cm^{-1} are attributed to symmetrical and asymmetrical vibrations of W^{6+}-O (stretching of OWO), while the bands at 272 and 320 cm^{-1} are attributed to deformation (WOW) [20].

MWCNT and graphene are carbonaceous materials, and D and G bands are the predominant features in the Raman spectrum. As depicted in Fig. 4c, d, D band at 1352 cm^{-1} characteristic of the symmetry breathing mode (A_1 g) involving the phonons near the boundary at point K. This mode is caused by structural defects and imperfections on the basal carbon plane. Otherwise, the G band at 1593 cm^{-1} corresponds to

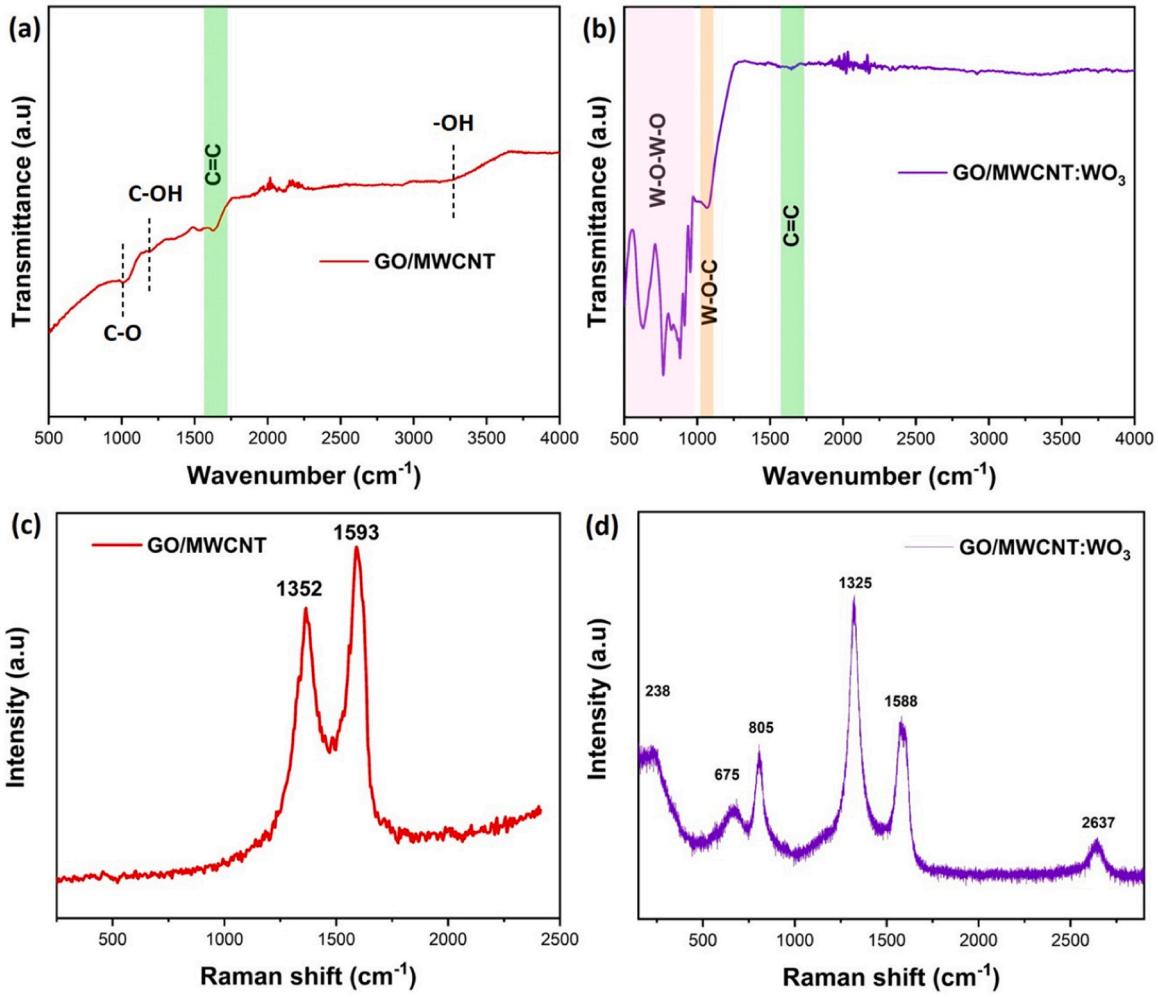

Fig. 4. (a, b) FTIR and (c, d) Raman spectra of GO/MWCNT and GO/MWCNT: WO_3 nanocomposites.

the first-order diffusion of the $E_{2\,g}$ mode at the Brillouin zone. However, the shift observed for D (1325 cm^{-1}) and G (1588 cm^{-1}) bands is due to the functionalization of WO_3 on the surface of GO/MWCNT. The same observation was reported by Wenjing Zeng et al. [21]. The I_D/I_G ratio of GO/MWCNT: WO_3 (1.36) is higher than GO/MWCNT (1.21), suggesting the creation of more defects and disorder onto the graphitic surface caused by the compounding with WO_3 nanostructures. In this study, the 2D band at 2600 cm^{-1} is a characteristic band confirming the exfoliated graphitic sheets in the nanocomposite [22]. The Raman spectrum further confirms the successful preparation of the ternary GO/MWCNT: WO_3 nanocomposite.

3.4. Photocatalytic activities

The photocatalysis is considered the best technique for the decomposition and degradation of pollutants worldwide. In this technique, an oxidation-reduction reaction occurs in the presence of light. As a result, highly reactive hydroxyl radicals (•OH) are produced. These hydroxyl radicals (•OH) are used to degrade the organic contaminants and convert them into CO_2, H_2O, and other inorganic compounds that are less toxic [23].

The photocatalytic activity of GO and prepared ternary nanocomposite GO/MWCNT: WO_3 was investigated using RhB as a model water pollutant. Fig. 5a, b depicts the UV–vis absorption spectra of Rhodamine after 240 min in the dark in the presence of catalyst GO and GO/MWCNT: WO_3. The spectra show two absorption peaks at 505 and 557 nm due to the corresponding absorption characteristics of completely de-ethylated and tetraethylated rhodamine B molecules [24]. It can be seen that the samples exhibit weak adsorption properties for RhB. The predominant absorption peak at 557 nm slowly decreases and reaches only (5 % for GO and 10 % for GO/MWCNT: WO_3) degradation after 240 min due to the less transformation of electron and hole. This result will help highlight the use of visible light for the successful degradation of RhB.

Fig. 5c, d show the absorption spectra of RhB solution under visible light irradiation using a solar simulator for different times in the presence of GO and GO/MWCNT: WO_3, respectively. It can be seen that the initial concentration of RhB decreases with irradiation time, and the rate of photodegradation strongly depends on the light and the catalyst. The RhB degradation rate for GO decreases slowly when subjected to visible light irradiation for 240 min due to the limitation of visible light absorption of GO. However, it has been noticed that the GO/MWCNT: WO_3 nanocomposite exhibits markedly improved photodegradation ability compared with GO.

This may be attributed to the synergistic reaction of the three components in the photocatalyst, which enhanced the photodegradation efficiency under visible light. The presence of WO_3 is beneficial to the improvement of absorbing light and generating more charge carriers [25]. The interaction between light and RhB molecules has been significantly improved due to the pivotal role of MWCNT in increasing the number of more active sites. Both GO, and MWCNT have large surface areas and sp^2 hybridization structures, which offer a unique network that delays charge recombination, promotes photogenerated charge separation, and improves charge transport ability [26].

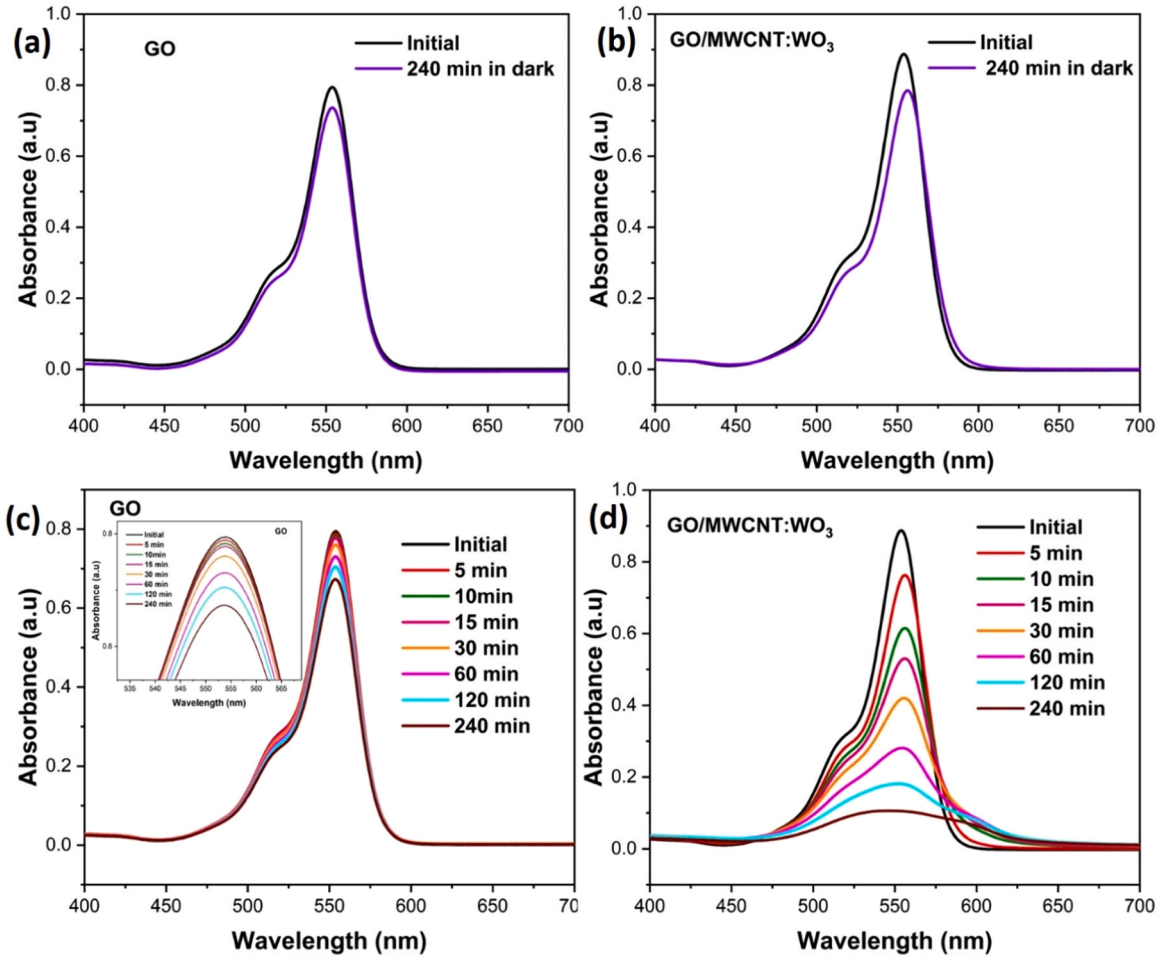

Fig. 5. Initial and after 240 min spectra of Rhodamine B (RhB) solution in which (a) GO and (b) GO/MWCNT: WO_3 nanocomposite was immersed, (c, d) Absorption spectra of RhB solutions after irradiation with visible light of a solar simulator for different times in the presence of GO and GO/MWCNT: WO_3 nanocomposite, respectively.

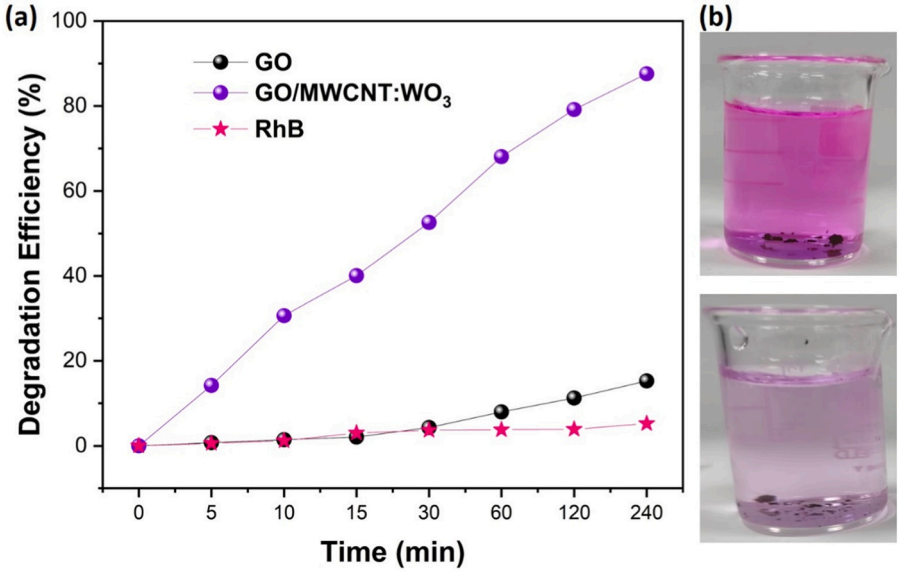

Fig. 6. (a) Degradation efficiency of RhB, GO, and GO/MWCNT: WO_3 nanocomposite; (b) RhB solution before and after irradiation under solar simulator light.

Table 1
Conditions and efficiency of nanocomposites based on WO_3, GO, and MWCNT used for RhB elimination from wastewater.

Photocatalyst	Method	Conditions	Deg., %	[Ref]
Graphene/ Ag_2S	Hydrothermal	Visible light, [Cat.] = 0.05 g, [RhB]= 5ppm, time-3h	83 %	[27]
PANI-$BiVO_4$-GO	Sonochemical deposition	Visible light, [Cat.] = 0.1 g, [RhB]= 10^{-5} M, time-2h	73 %	[28]
GO/WO_3/TiO_2	Sol-gel	visible light, [Cat.] = 0.15 g [RhB]= 3.10^{-5} M, time-3h	70 %	[29]
TiO_2:N/ MWCNT	Direct mixing	UV irradiation, [RhB]= 100 μM, T = 25 C, time-5h	70 %	[30]
GO/MWCNT: WO_3	Chemical process	Visible light, [Cat] = 0.5 mg, [RhB]= 10^{-5} M, time-4h	85 %	This work

The degradation of dye was evaluated by taking samples after a specific interval of time (Fig. 6a). The performance of GO and GO/MWCNT: WO_3 for pollutant degradation was calculated by using the following formula of degradation efficiency (%):

$$\text{Degradation efficiency}(\%) = \frac{(C_0 - C)}{C_0} \times 100$$

Where, C_0 represents dye's initial absorbance at λ_{max} and C is the absorbance of dye at an instant of time. The results revealed the reduction of RhB concentration during the photoreduction process. After 240 min, in the presence of sunlight, the dye degradation processes started, which resulted in the color change of solution as depicted in Fig. 6b, indicating that approximately 85 % of RhB has been degraded in the presence of GO/MWCNT: WO_3 catalyst. The photocatalytic degradation of Rhodamine-B in water under visible light irradiation was significantly enhanced using the GO/MWCNT: WO_3 nanocomposite, achieving an 85 % degradation rate compared to only 10 % by GO alone, highlighting its potential for environmental remediation. Compared to previous studies (Table 1) on the photocatalytic performance of nanocomposites for RhB degradation, the catalyst in this work demonstrates remarkable efficiency.

Fig. 7 illustrates the photocatalytic activity of the prepared photocatalysts concerning the degradation of Rhodamine B (RhB) dye under visible light. Upon exposing the dye solution to solar light, electrons that remain in the valence band (VB) of tungsten trioxide absorb light energy and are excited into the conduction band (CB), while holes remain behind. During this process, electron-hole pairs are formed owing to white light irradiation. The excited electrons react with oxygen to form superoxide ($O_2^{-\bullet}$) radicals and the holes participate in the reaction with water to generate hydroxyl (•OH) radicals. These radicals are critical in determining photocatalytic activity as they help the degradation of organic dyes into water and carbon dioxide (CO_2). Electron-hole (e^--h^+) pairs must have a high recombination time to generate more radicals. In our novel ternary composites, GO enhances the delocalization of photogenerated electrons by its π-network, increasing the recombination period. At the same time, MWCNTs create space between GO sheets, preventing them from aggregating and increasing the number of active sites available for photocatalytic performance [31]. With these advantages, tungsten trioxide nanostructures have been incorporated into MWCNTs and GO, forming a semiconductor heterojunction that further prolongs the recombination time of electron-hole pairs and improves photodegradation efficiency.

4. Conclusion

An efficient visible-light photocatalyst was prepared using a simple and cost-effective method. The structural and morphological investigations confirmed the incorporation of nanostructured WO_3 into the GO/MWCNT matrix. Moreover, the chemical bonding was confirmed using the FTIR and Raman techniques. The photocatalytic study highlighted the degradation efficiency of RhB (85 %) in 240 min under visible light irradiation compared with GO (10 %). This enhancement is due to the WO_3 light absorption properties and the introduction of MWCNT, which provide more active sites and surface area for the interaction with RhB. Combining the three components improved the charge-transport property and promoted the separation of photogenerated charge carriers. The results show that GO/MWCNT: WO_3 composite has great potential for wastewater treatment.

CRediT authorship contribution statement

Enculescu Monica: Validation, Supervision, Funding acquisition, Formal analysis. **Baitoul Mimouna:** Visualization, Validation, Software, Resources. **Matei Elena:** Visualization, Validation, Supervision, Methodology. **Hatel Rhizlane:** Writing – original draft, Validation,

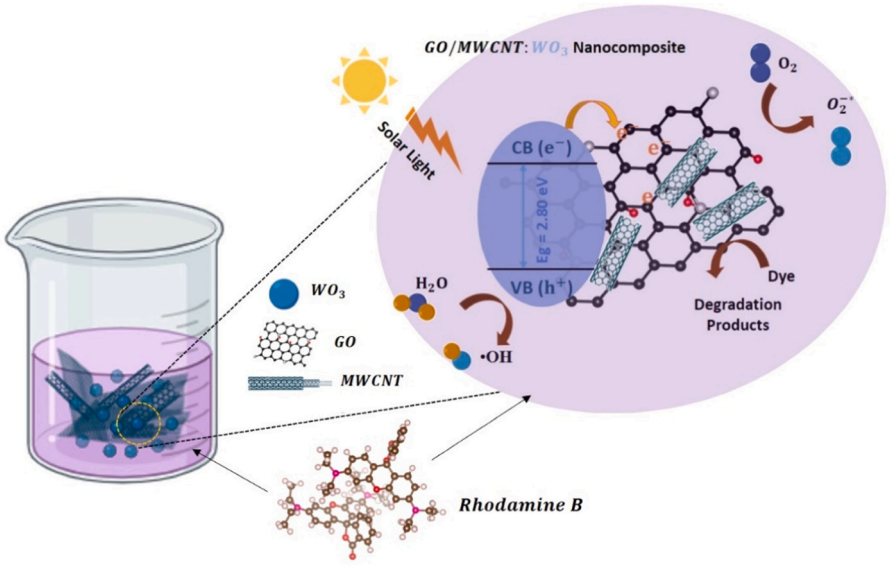

Fig. 7. Schematic representation of the mechanism of photocatalytic activity of GO/MWCNT: WO_3 nanocomposite under solar light irradiation.

Resources, Investigation, Formal analysis, Data curation, Conceptualization. **Boukhoubza Issam:** Visualization, Methodology, Investigation, Formal analysis. **Derkaoui Issam:** Visualization, Validation, Resources, Methodology. **Basyooni-M. Kabatas Mohamed A.:** Writing – review & editing, Visualization, Validation, Investigation.

Declaration of Competing Interest

The authors declare that they have no known competing financial interests or personal relationships that could have appeared to influence the work reported in this paper

Acknowledgments

Thanks to the National Institute of Materials Physics (Romania), the Romanian Ministry of Foreign Affairs, and the Agence Universitaire de la Francophonie for the Eugen Ionescu research. E.M. acknowledges financial support from the EU under Romanian Recovery and Resilience Plan PNRR, Pillar III, Component C9-I8, contract nr.760083/23.05.2023, and M.E. acknowledges support from the National Institute of Materials Physics Core Program, granted by the Romanian Ministry of Research, Innovation, and Digitalization under Project PC1-PN23080101.

Data Availability

Data will be made available on request.

References

[1] N. Kitchamsetti, M.S. Ramteke, S.R. Rondiya, S.R. Mulani, M.S. Patil, R.W. Cross, N.Y. Dzade, R.S. Devan, DFT and experimental investigations on the photocatalytic activities of NiO nanobelts for removal of organic pollutants, J. Alloy. Compd. 855 (2021) 157337.
[2] R. Al-Tohamy, S.S. Ali, F. Li, K.M. Okasha, Y.A.G. Mahmoud, T. Elsamahy, H. Jiao, Y. Fu, J. Sun, A critical review on the treatment of dye-containing wastewater: ecotoxicological and health concerns of textile dyes and possible remediation approaches for environmental safety, Ecotoxicol. Environ. Saf. 231 (2022) 113160.
[3] P. Bartasun, H. Cieśliński, A. Bujacz, A. Wierzbicka-Woś, J. Kur, A study on the interaction of rhodamine B with methylthioadenosine phosphorylase protein sourced from an Antarctic soil metagenomic library, PLoS One 8 (1) (2013) e55697.
[4] S. Duman, E. Yilmaz, M. Soylak, Solid phase microextraction of rhodamine B in cosmetic samples using ZnS@GO@WMCNTs nanocomposite with spectrophotometric detection, Microchem. J. 199 (2024) 110214.
[5] A. Saravanan, P.S. Kumar, S. Jeevanantham, S. Karishma, B. Tajsabreen, P. R. Yaashikaa, B. Reshma, Effective water/wastewater treatment methodologies for toxic pollutants removal: processes and applications towards sustainable development, Chemosphere 280 (2021) 130595.
[6] H. Kumari, Sonia, Suman, R. Ranga, S. Chahal, S. Devi, S. Sharma, S. Kumar, P. Kumar, S. Kumar, A. Kumar, R. Parmar, A review on photocatalysis used for wastewater treatment: dye degradation, Water Air Soil Pollut. 234 (6) (2023) 349.
[7] G. Ramalingam, N. Perumal, A.K. Priya, S. Rajendran, A review of graphene-based semiconductors for photocatalytic degradation of pollutants in wastewater, Chemosphere 300 (2022) 134391.
[8] I.A. Shah, M. Bilal, I.W. Almanassra, I. Ihsanullah, A comprehensive review of graphene oxide-based membranes for efficient dye removal from water sources, Sep. Purif. Technol. 330 (2024) 125277.
[9] A. Abidli, Z.B. Rejeb, A. Zaoui, H.E. Naguib, C.B. Park, Comprehensive insights into the application of graphene-based aerogels for metals removal from aqueous media: Surface chemistry, mechanisms, and key features, Adv. Colloid Interface Sci. (2024) 103338.
[10] G. Ramalingam, N. Perumal, A.K. Priya, S. Rajendran, A review of graphene-based semiconductors for photocatalytic degradation of pollutants in wastewater, Chemosphere 300 (2022) 134391.
[11] C. Wang, M. Cao, P. Wang, Y. Ao, J. Hou, J. Qian, Preparation of graphene–carbon nanotube–TiO_2 composites with enhanced photocatalytic activity for the removal of dye and Cr (VI), Appl. Catal. A: Gen. 473 (2014) 83–89.
[12] V. Dutta, S. Sharma, P. Raizada, V.K. Thakur, A.A.P. Khan, V. Saini, A.M. Asiri, P. Singh, An overview on WO_3 based photocatalyst for environmental remediation, J. Environ. Chem. Eng. 9 (1) (2021) 105018.
[13] H. Saleem, M. Haneef, H.Y. Abbasi, Synthesis route of reduced graphene oxide via thermal reduction of chemically exfoliated graphene oxide, Mater. Chem. Phys. 204 (2018) 1–7.
[14] R. Hatel, M. Baitoul, Nanostructured Tungsten Trioxide (WO_3): synthesis, structural and morphological investigations, J. Phys.: Conf. Ser. 1292 (2019) 012014.
[15] S. Ramesh, A. Sivasamy, H.S. Kim, J.H. Kim, High-performance N-doped MWCNT/GO/cellulose hybrid composites for supercapacitor electrodes, RSC Adv. 7 (78) (2017) 49799–49809.
[16] A.C. Marques, L. Santos, M.N. Costa, J.M. Dantas, P. Duarte, A. Gonçalves, R. Martins, C.A. Salgueiro, E. Fortunato, Office paper platform for bioelectrochromic detection of electrochemically active bacteria using tungsten trioxide nanoprobes, Sci. Rep. 5 (1) (2015) 9910.
[17] R. Hatel, M. Baitoul, A novel approach to synthesize nanostructured WO_3 and graphene/WO_3 nanocomposites: structural and morphological investigations, Mater. Chem. Phys. 225 (2019) 169–173.
[18] S. Cheng, X. Zeng, P. Liu, One-step synthesis of magnetic N-doped carbon nanotubes derived from waste plastics for effective Cr (VI) removal, Arab. J. Chem. 17 (10) (2024) 105956.
[19] K. Thummavichai, Y. Xia, Y. Zhu, Recent progress in chromogenic research of tungsten oxides towards energy-related applications, Prog. Mater. Sci. 88 (2017) 281–324.
[20] T. Singh, R. Müller, J. Singh, S. Mathur, Tailoring surface states in WO_3 photoanodes for efficient photoelectrochemical water splitting, Appl. Surf. Sci. 347 (2015) 448–453.
[21] W. Zeng, M. Gao, K. Liu, C. Li, N. Cao, X. Zhao, J. Feng, Y. Ren, T. Wei, Boosting charge separation and surface defects for superb photocatalytic activity of magnesium oxide/graphene nanosheets, Appl. Surf. Sci. 535 (2021) 147658.
[22] S.S. Sukumaran, C.R. Rekha, A.N. Resmi, K.B. Jinesh, K.G. Gopchandran, Raman and scanning tunneling spectroscopic investigations on graphene-silver nanocomposites, J. Sci.: Adv. Mater. Devices 3 (3) (2018) 353–358.
[23] S.K. Bhunia, N.R. Jana, Reduced graphene oxide-silver nanoparticle composite as visible light photocatalyst for degradation of colorless endocrine disruptors, ACS Appl. Mater. Interfaces 6 (22) (2014) 20085–20092.
[24] S. Singh, G. Hitkari, G. Pandey, Synthesis, characterization of Fe_3O_4, $CoFe_2O_4$ nanomaterials and its application in photodegradation of rhodamin B dye, Synthesis 4 (5) (2017) 3966–3970.
[25] Q. Qiu, P. Zhu, Y. Liu, T. Liang, T. Xie, Y. Lin, Highly efficient In_2S_3/WO_3 photocatalysts: Z-scheme photocatalytic mechanism for enhanced photocatalytic water pollutant degradation under visible light irradiation, RSC Adv. 11 (6) (2021) 3333–3341.
[26] S. Srinithi, V. Balakumar, T.W. Chen, S.M. Chen, M. Akilarasan, B.S. Lou, J. Yu, In-situ fabrication of TiO_2-MWCNT composite for an efficient electron transfer photocatalytic rhodamine B dye degradation under UV–visible light, Diam. Relat. Mater. 138 (2023) 110245.
[27] H. Wenda, Z. Leihong, Zh Yuting, Z. Xin, D. Lvzhuo, W. Sisi, H. Yiming, Preparation and photocatalytic activity of graphene-modified Ag2S composite, J. Exp. Nanosci. 11 (6) (2016) 433–444.
[28] M.R.U.D. Biswas, K.Y. Cho, J.D. Na, W.C. Oh, Highly electro-conductive graphene-decorated PANI-BiVO4 polymer-semiconductor nanocomposite with outstanding photocatalytic performance, Mater. Sci. Eng., B 251 (2019) 114469.
[29] X. Liu, C. Chen, X.A. Chen, G. Qian, J. Wang, C. Wang, Z. Cao, Q. Liu, WO_3 QDs enhanced photocatalytic and electrochemical perfomance of GO/TiO2 composite, Catal. Today 315 (2018) 155–161.
[30] A. Udrescu, S. Florica, M. Chivu, I. Mercioniu, E. Matei, M. Baibarac, Rhodamine B photodegradation in aqueous solutions containing nitrogen doped TiO2 and carbon nanotubes composites, Molecules 26 (23) (2021) 7237.
[31] C. Wang, M. Cao, P. Wang, Y. Ao, J. Hou, J. Qian, Preparation of graphene-carbon nanotube-TiO_2 composites with enhanced photocatalytic activity for the removal of dye and Cr (VI), Appl. Catal. A: Gen. 473 (2014) 83–89.